Search for trapped antihydrogen in ALPHA[1]

N. Madsen, G.B. Andresen, M.D. Ashkezari, M. Baquero-Ruiz, W. Bertsche, P.D. Bowe, C. Bray, E. Butler, C.L. Cesar, S. Chapman, M. Charlton, J. Fajans, T. Friesen, M.C. Fujiwara, D.R. Gill, J.S. Hangst, W.N. Hardy, M.E. Hayden, A.J. Humphries, R. Hydomako, S. Jonsell, L.V. Jørgensen, L. Kurchaninov, R. Lambo, S. Menary, P. Nolan, K. Olchanski, A. Olin, A. Povilus, P. Pusa, F. Robicheaux, E. Sarid, S. Seif El Nasr, D.M. Silveira, C. So, J.W. Storey, R.I. Thompson, D.P. van der Werf, J.S. Wurtele, and Y. Yamazaki

Abstract: Antihydrogen spectroscopy promises precise tests of the symmetry of matter and antimatter, and can possibly offer new insights into the baryon asymmetry of the universe. Antihydrogen is, however, difficult to synthesize and is produced only in small quantities. The ALPHA collaboration is therefore pursuing a path towards trapping cold antihydrogen to permit the use of precision atomic physics tools to carry out comparisons of antihydrogen and hydrogen. ALPHA has addressed these challenges. Control of the plasma sizes has helped to lower the influence of the multipole field used in the neutral atom trap, and thus lowered the temperature of the created atoms. Finally, the first systematic attempt to identify trapped antihydrogen in our system is discussed. This discussion includes special techniques for fast release of the trapped antiatoms, as well as a silicon vertex detector to identify antiproton annihilations. The silicon detector reduces the background of annihilations, including background from antiprotons that can be mirror trapped in the fields of the neutral atom trap. A description of how to differentiate between these events and those resulting from trapped antihydrogen atoms is also included.

PACS Nos: 25.43.+t, 34.80.Lx, 36.10.–k, 37.10.Gh

Résumé : La spectroscopie de l'anti-hydrogène promet des tests précieux de la symétrie entre matière et antimatière dans l'univers. Cependant, l'anti-hydrogène est difficile à synthétiser et il n'est produit qu'en petite quantité. Le groupe de collaborateurs ALPHA poursuit donc des travaux pour capturer de l'anti-hydrogène froid afin de permettre l'utilisation d'outils précis de mesure en physique atomique pour comparer l'anti-hydrogène avec l'hydrogène. Nous montrons comment ALPHA s'est attaqué à cette tâche et comment le contrôle du volume de plasma a aidé à diminuer l'influence des champs multipolaires utilisés dans le piège pour atomes neutres et ainsi abaisser la température des atomes produits. Finalement, nous discutons le premier essai systématique pour identifier l'anti-hydrogène piégé dans notre système. Ceci inclut des techniques spéciales pour relâcher rapidement les anti-atomes piégés, ainsi qu'un détecteur au silicium pour identifier l'annihilation de l'anti-proton. Nous avons utilisé le détecteur au silicium pour réduire le fond d'annihilation, incluant celui produit par les anti-protons qui peuvent être dans le piège miroir des champs du piège à atomes neutres. Nous décrivons aussi comment nous pouvons différentier entre ces événements et ceux qui résultent des atomes d'anti-hydrogène piégés.

[Traduit par la Rédaction]

Received 18 July 2010. Accepted 30 August 2010. Published on the NRC Research Press Web site at cjp.nrc.ca on 21 December 2010.

N. Madsen,[2] W. Bertsche, E. Butler, M. Charlton, A.J. Humphries, S. Jonsell, L.V. Jørgensen, and D.P. van der Werf. Department of Physics, Swansea University, Swansea SA2 8PP, UK.
G.B Andresen, P.D. Bowe, and J.S. Hangst. Department of Physics and Astronomy, Aarhus University, 8000 Aarhus C, Denmark.
M.D. Ashkezari and M.E. Hayden. Department of Physics, Simon Fraser University, Burnaby, BC V5A 1S6, Canada.
M. Baquero-Ruiz, C. Bray, S. Chapman, J. Fajans, A. Povilus, C. So, and J.S. Wurtele. Department of Physics, University of California at Berkeley, Berkeley, CA 94720-7300, USA.
C.L. Cesar and R. Lambo. Instituto de Física, Universidade Federal do Rio de Janeiro, Rio de Janeiro 21941-972, Brazil.
T. Friesen, R. Hydomako, and R.I. Thompson. Department of Physics and Astronomy, University of Calgary, Calgary, AB T2N 1N4, Canada.
M.C. Fujiwara, D.R. Gill, L. Kurchaninov, K. Olchanski, A. Olin, and J.W. Storey. TRIUMF, 4004 Wesbrook Mall Vancouver, BC V6T 2A3, Canada.
W.N. Hardy and S.S. El Nasr. Department of Physics and Astronomy, University of British Columbia, Vancouver, BC V6T 1Z1, Canada.
S. Menary. Department of Physics, York University, Toronto, ON M3J 1P3, Canada.
P. Nolan and P. Pusa. Department of Physics, University of Liverpool, Liverpool L69 7ZE, UK.
F. Robicheaux. Department of Physics, Auburn University, Auburn, AL 36849-5311, USA.
E. Sarid. Department of Physics, NRCN-Nuclear Research Center Negev, Beer Sheva, IL-84190, Israel.
D.M Silveira and Y. Yamazaki. Atomic Physics Laboratory, RIKEN, Saitama 351-0198, Japan.

[1]This paper was presented at the International Conference on Precision Physics of Simple Atomic Systems, held at École de Physique, les Houches, France, 30 May – 4 June, 2010.

[2]Corresponding author (e-mail: Niels.Madsen@cern.ch).

Fig. 1. Schematic of the ALPHA setup. Antiprotons enter from the left and positrons from the right. The various parts of the apparatus are discussed throughout the text.

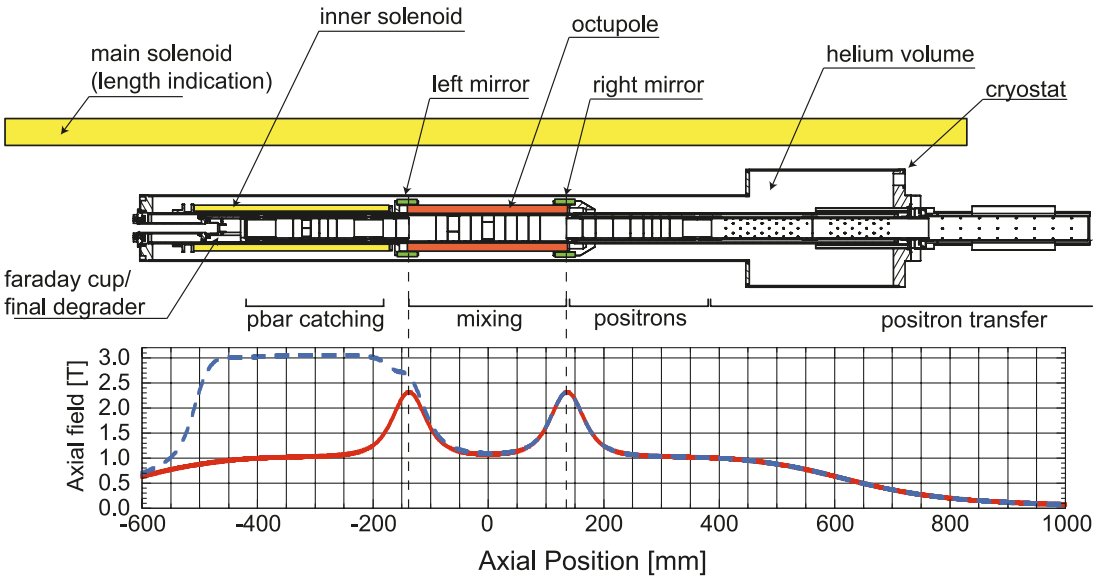

1. Introduction

Antihydrogen, the antimatter counterpart of hydrogen, holds the promise of precise tests of the CPT theorem and the weak equivalence principle through direct comparisons with hydrogen [1]. Since the first formation of cold antihydrogen potentially amenable to such studies by the ATHENA and ATRAP collaborations working at CERN in 2002 [2, 3], several groups have pursued comparisons in various ways, though none have been carried out thus far. For high precision in spectroscopic studies it is thought advantageous to first trap the antihydrogen atoms to allow for accumulation of these very rare atoms, as well as to ensure longer interrogation times. Here we describe the progress of the ALPHA collaboration, a successor of the ATHENA collaboration, also working at CERN, towards this first goal. Trapping of antihydrogen is complicated by the fact that antiprotons can only be created at high energy and there are no readily available methods for cooling the antihydrogen atoms. We discuss how ALPHA has approached this challenge, how conditions have been reached where one could expect to trap some antihydrogen atoms, and the results of a systematic effort yielding the first few candidates events.

Antihydrogen, like hydrogen, can be trapped via its magnetic dipole moment. The potential energy U of a dipole of moment $\bar{\mu}$ in a magnetic field $\bar{B}$ is

$$U = -\bar{\mu}\bar{B} \tag{1}$$

which means that, assuming the dipole is a paramagnet, i.e., it orients itself parallel to $\bar{B}$, the dipole can be trapped in a three-dimensional magnetic minimum. For (anti)hydrogen in the ground state, $\bar{\mu}$ is the Bohr magneton and we find a trap depth of about 0.7 K/T. ALPHA has constructed a state-of-the-art set of super-conducting magnets to form such a minimum, creating an Ioffe–Pritchard-like geometry, where two coaxial separated short solenoids (called mirror coils) form the axial magnetic minimum and a coaxial octupole is used to form the transverse minimum [4]. The resulting trap depth is about 1 T. In earlier experiments by the ALPHA predecessor ATHENA, as well as the competing experiment ATRAP, it was found that antihydrogen was formed at temperatures orders of magnitude larger those that can be held in this depth [5, 6]. ALPHA has therefore expended considerable effort on reducing the temperature of the synthesized antihydrogen as will be detailed in the following.

The introduction of a magnetic minimum adds an additional complication to the trapping of antihydrogen. Magnetic fields that break the rotational symmetry of the Penning–Malmberg trap used (see Sect. 2) can cause both direct losses of the confined plasmas as well as increased diffusive losses [7]. We have also observed that such processes, perhaps unsurprisingly, lead to heating of the plasmas. Since the antihydrogen atoms are quickly lost, no readily available cooling exists that could assist the trapping process. Therefore, antihydrogen must be produced inside the magnetic minimum at the required low temperatures. It was thus essential that the magnetic-minimum trap caused as little perturbation to the trapped charged particles as possible, which is why an octupole was chosen to form the transverse minimum rather than the more commonly used quadrupole.

2. Antihydrogen formation

In the experiments discussed here, antihydrogen is made by merging plasmas of cold antiprotons and positrons. This method has proven itself to be a robust and easy way to produce large amounts of antihydrogen in both the ALPHA and the former ATHENA experiments [8, 9]. All charged particle traps used are of the Penning–Malmberg type where a strong axial magnetic field confines the charged particles radially and axial electric fields confine them axially. The axial magnetic field is generated by an external solenoidal magnet and is typically 1 T. The axial electric fields are generated by individually excitable coaxial electrodes. The

Fig. 2. Azimuthal projections of the antiproton annihilation vertex distributions during mixing with (*a*) no neutral atom trap and (*b*) the full trap. Corresponding *z*-ϕ distributions. Corresponding axial (*z*) distributions. (*f*) Dashed (red): fit to the distribution, see text; dot-dashed (green) peaks in fit. The shaded area marks the three layer part of the detector used for tracking. Left of this area the detector has only one layer of silicon. The slight asymmetry in the axial distributions (in particular the tails) is due to the lower reconstruction efficiency outside the three layer section. For clarity the plots have been normalized to have the same total number of events. The total numbers of events with and without the neutral trap were 6830 and 26823, respectively. The zero axial position is the center of the neutral atom trap.

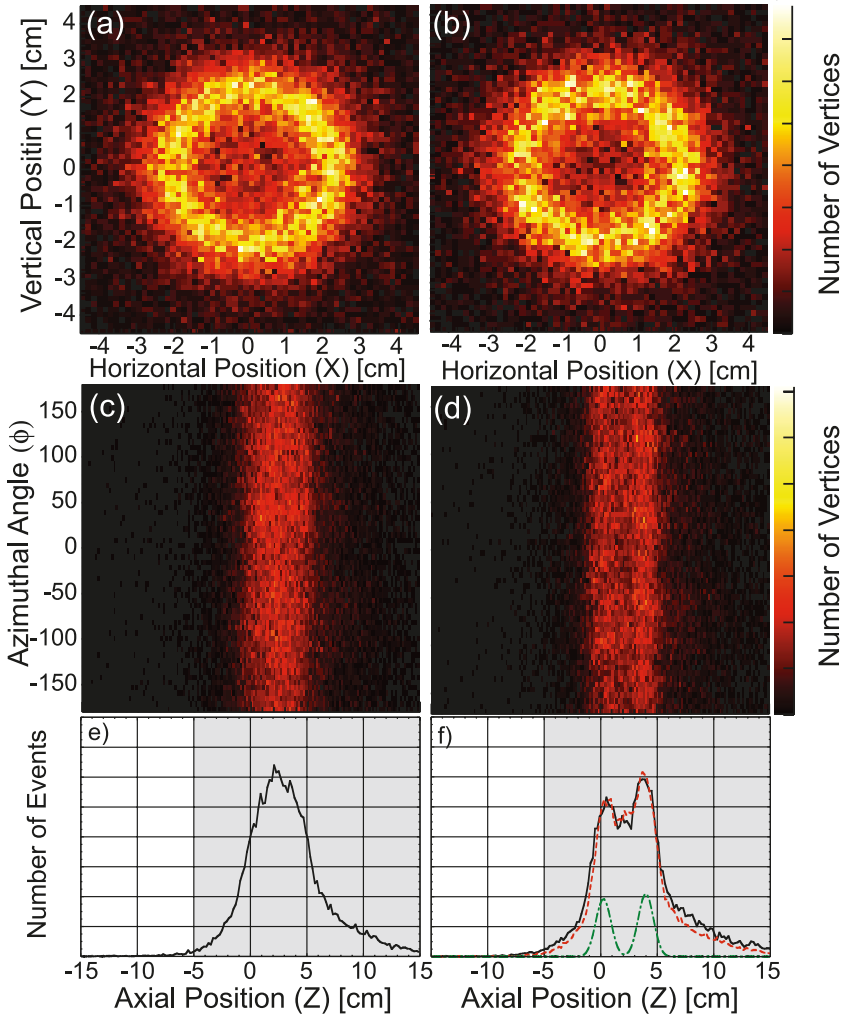

main apparatus in which antihydrogen is formed (Fig. 1), consists of two main regions; one for capture and cooling of the antiprotons, and one for making, and eventually trapping, antihydrogen. The latter is also used for capturing positrons that originate from an external Surko-type buffer gas positron accumulator [10]. The magnetic-minimum trap described earlier is superposed on this central region. The trap system is cooled to $\sim$8 K by the same cryostat that is used to cool the superconducting magnetsthat form the trap for antihydrogen.

Antiprotons are delivered by CERN's unique antiproton decelerator (AD) in batches of about 4×10^7 antiprotons every 100 s at 5.3 MeV [11]. The kinetic energy of the antiprotons is degraded by passing them through a thin, $\sim$0.2 mm aluminium foil and they are then dynamically trapped using potentials of a few kiloVolts. Before capture, a small, typically about 2×10^7, batch of electrons has been loaded into the capture region. The electrons originate from an electron gun located to the outside right of Fig. 1. The gun is mounted on a translation device that also holds a short cylindrical electrode to allow positrons to transfer from the accumulator further to the right. Also mounted on the translator is an imaging micro-channel-plate (MCP) phosphor assembly, which, together with an externally mounted camera, allows imaging of electrons, positrons, and antiprotons [12], thus allowing us to measure their radial density profiles.

The antiprotons are left to cool on the electrons for typically 80 s. We then apply a so-called rotating wall (RW), which is an azimuthally rotating dipole electric field, generated by imposing appropriately phase-shifted sinusoidal signals on each segment of an azimuthally segmented electrode. The RW allows us to compress the antiproton–electron mixture such that it will be less sensitive to the transverse magnetic fields imposed by the magnetic-minimum trap and ensures a better physical overlap with the positrons [13]. The mixture is transported to the mixing region. In the meantime, positrons have been transferred from

Fig. 3. Plots of the electric and magnetic fields used to create antihydrogen in a minimum-*B* neutral atom trap. The lower plot shows the axial magnetic fields with (dot-dash) and without (long dash) the magnetic mirrors and the electric potential on axis at the beginning (solid line) and the end (short dash) of the mixing cycle. The black ellipse indicates the initial position and energy of the antiprotons ($\bar{p}$). The top plot shows the corresponding total electric field strength versus radius and axial position at the end of the mixing.

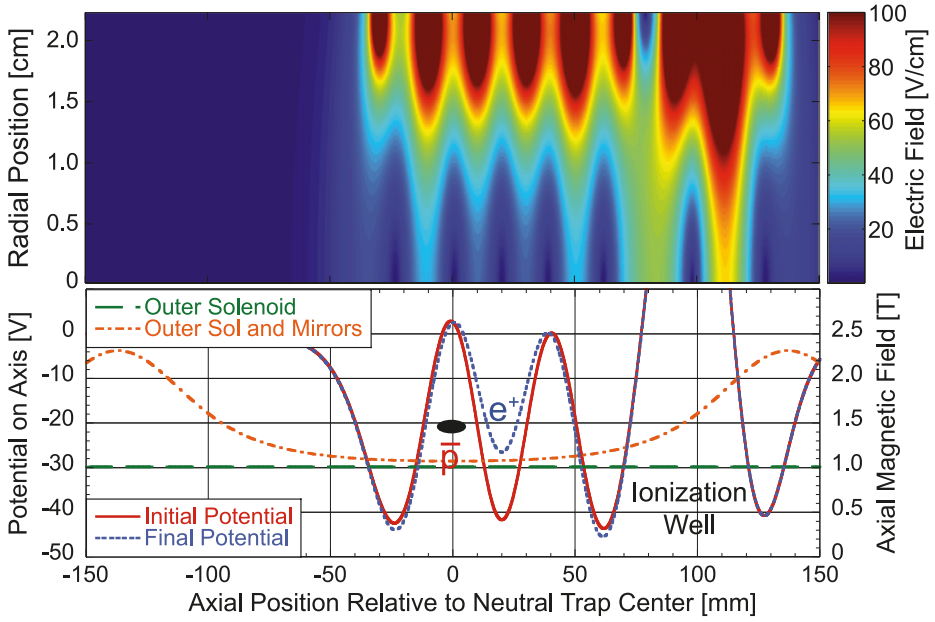

Fig. 4. Antiprotons lost as a function of trap depth. Annihilation events are counted while the trap depth is lowered over 100 ms. The detector has a 25%±5% absolute efficiency for detecting an antiproton annihilation. The graph shows how many particles escaped at each point in this process. The temperature is extracted by fitting the release of the first approximately two hundred escaping particles, and the fit gave 219±33 K. The counting uncertainty is purely statistical, and the extracted temperature has not been corrected for adiabatic cooling nor space charge (see text). The horizontal uncertainty represents the energy resolution of the measurement.

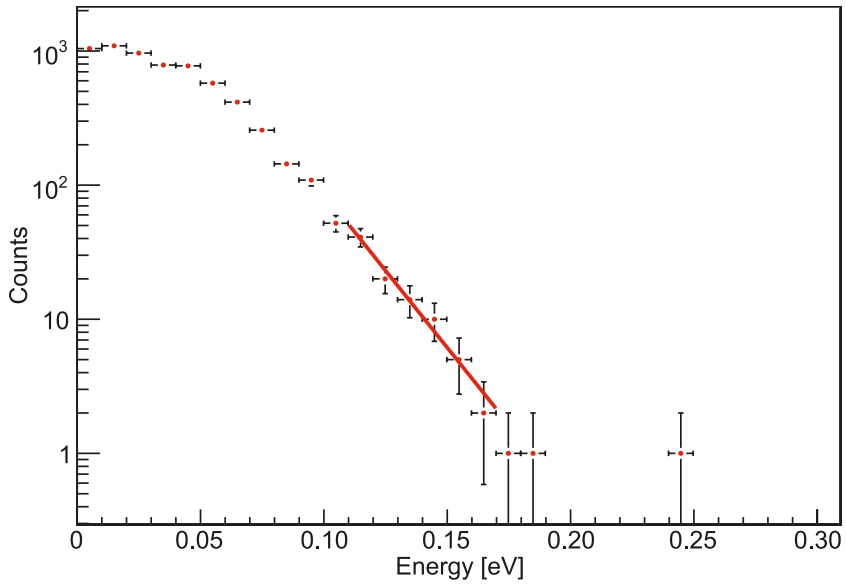

the accumulator to the center of the trap, where their radial extent has also been reduced by a second RW. After letting both the positrons and antiprotons cool for about a minute, the electrons are removed from the antiproton cloud by a series of electric pulses that leave their shared trap open for about 100 ns; long enough for the electrons to escape, but short enough for the antiprotons to remain.

Finally, the antiprotons and positrons are slowly merged. It is imperative that this process does not heat any of the species as that would result in hot antihydrogen. In the 2009 experimental search for trapped antihydrogen, we measured temperatures of the positrons of ∼170 K and antiprotons of ∼300 K. Based on a code used by Robicheaux to calculate cooling and recombination rates [14], we expect that, for both species, at such temperatures the antiprotons are expected to reach thermal equilibrium with the positrons before antihydrogen is formed. Currently, the positron temperature is the limiting factor for producing colder antihy-

Fig. 5. Examples of reconstruction of (*a*) an antihydrogen annihilation and (*b*) a cosmic ray event. The straight line pieces surrounding the centre are the silicon modules seen on the short edge. The ring in the centre is the inner wall of the electrodes. The fat round dots indicate where a module has been triggered and the curved lines are the reconstructed tracks. The diamond marks the reconstructed vertex (see text).

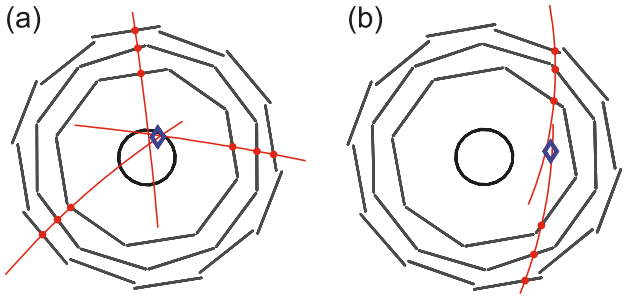

drogen. These temperatures are still much larger than what can be held by our trap, but if antihydrogen is produced at 170 K a small fraction will be cold enough to be trappable.

We can measure the anitproton annihilation vertices using a purpose-built three-layer silicon vertex detector (see Sect. 4). When antihydrogen is formed with the magnetic trap turned off we observe a similar spatial distribution of the antiproton annihilations as did ATHENA (see Fig. 2). The distribution is smooth and azimuthally symmetric and the annihilations coincident with the trap walls of $\sim$22 mm radius, supporting the expectation that the neutral antihydrogen emerges without any spatially preferred direction. The distribution is not perfectly isotropic as (*i*) the plasmas are rotating due to the crossed electric and magnetic fields that may add significant transverse velocity to the antihydrogen, and (*ii*) the axial and transverse temperatures are not always in equilibrium. This was studied in detail in ref. 5, and led to the conclusion that antihydrogen created by launching antiprotons into a positron plasma at electron-Volt energies caused the antihydrogen formed to be too hot for trapping.

When antihydrogen is formed inside the neutral trap the octupole significantly influences the outcome. In this case it is necessary that the radial extent of the particle ensembles is smaller than the so-called critical radius, a dynamic aperture introduced by the superposition of an octupole on a Penning–Malmberg trap [15]. Particles beyond this critical radius will be lost. When antihydrogen is formed within the neutral trap, weakly bound antihydrogen may field-ionize on the fields in the trap (see e.g., Fig. 3). As described in detail in ref. 9, antihydrogen thus field-ionized may leave its antiproton beyond the critical radius, causing it to be lost immediately along the field-line that it finds itself on following the field-ionization. This process causes two axial peaks to form, and the appearance of azimuthal peaks corresponding to the rotational symmetry of the octupole magnet. When the neutral trap is energized, the annihilation triggers measured by the detector originate from a mixture of two event-types. The first is antihydrogen that drifts from its creation point to the wall and annihilates as antihydrogen. The second is antihydrogen that is too weakly bound to survive the drift to the wall, and field-ionizes at a point on the way, where its antiproton will be lost if the points falls beyond the aforementioned critical radius. By analysing the annihilation vertex distribution we can distringuish between the two event types. Only antihydrogen that does not field-ionize is potentially trappable, and for the experiments detailed in this article $\sim$80% of the annihilation detector triggers were caused by such directly lost, and potentially trappable, antihydrogen.

3. Particle temperatures

Antihydrogen will inherit its temperature from the antiprotons, since the relatively low mass of the captured positron means that it contributes almost nothing to the final kinetic energy of a newly formed antihydrogen atom. The positrons, however, do cool through the emission of synchrotron radiation in the cryogenic environment of the traps used. It was originally assumed that the antiprotons in the merged plasma scheme would first cool to the temperature of the self-cooling positrons, and then form antihydrogen. Measurements from ATHENA demonstrated that this was not the case when the antiprotons were injected with the then-typical energy of up to 10 eV relative to the positron plasma [5]. In recognition of these results we now introduce the antiprotons very carefully into the positron plasma by a minimum amount of manipulation of the potentials, as shown, for example, in Fig. 3.

We can directly measure the temperature of all particle species by gently lowering the confining potential while counting the number of escaping particles, and thus measuring the exponential tail of the Boltzmann distribution [16, 17]. For this to work, it is important that we be able to count very low numbers of particles, as the space charge field of the particle clouds as well as the changes in the cloud during ejection can mask this information. Figure 4 shows a temperature measurement of a typical ensemble of antiprotons used for the trapping experiments described here. Particle-in-cell simulations of our ejections show that the various effects such as space charge and adiabatic cooling leads us to *overestimate* our temperatures by up to 40%. The temperatures given here are the raw data, without compensation for any such effects.

4. Detecting antiproton annihilations

When ejecting antiprotons axially from the trap we can detect them by registering the resulting pions passing through externally mounted scintillators connected to photomultiplier tubes. However, to enhance our ability to reject cosmic events, and to distinguish antihydrogen from antiprotons, we have installed an annihilation detector similar to that used by ATHENA [2, 5]. The annihilation detector consists of three layers of double-sided silicon strip detectors that can detect the position of a passing charged particle [18]. By reconstructing the tracks from the charged pions we can, once there are enough of these (minimum two), reconstruct the annihilation vertex of the antiproton whose annihilation gave rise to the detected charged pions. The magnets for the magnetic-minimum trap added additional material between the vacuum in the trap and the detector, such that it is not possible to detect the gamma ray photons from positron annihilations as performed by ATHENA [2].

Figure 5 shows two examples of events detected by the annihilation detector. The figure shows (*a*) a reconstructed antihydrogen event, where three charged pions were de-

Fig. 6. Currents in the octupole and the two mirror coils measured as a function of time after the fast de-energization of the magnets has been triggered. The shaded area shows the window during which we searched for annihilations. The time constants have been determined by exponential fits to the currents.

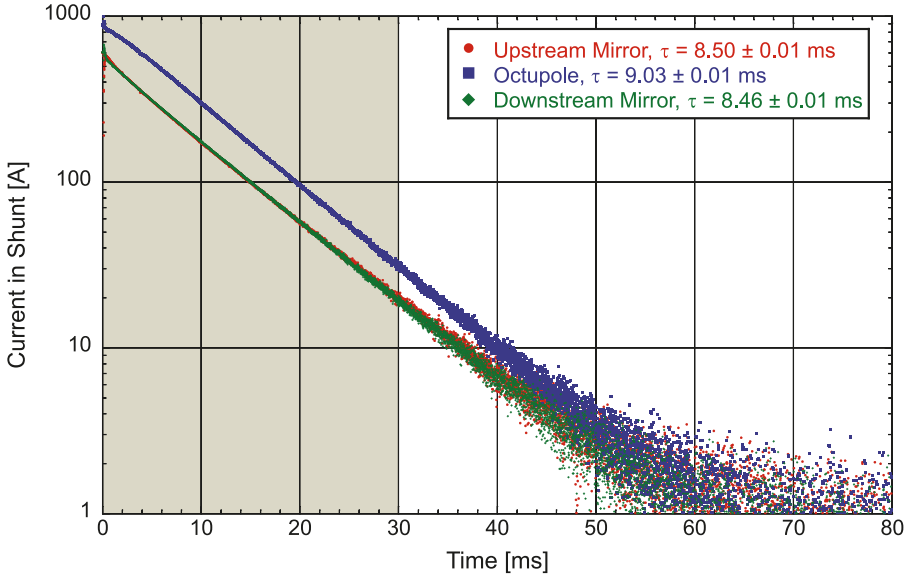

Fig. 7. Measured distributions of (*a*) the number of identified charged particle tracks, (*b*) the radial coordinate of the vertex, and the squared residual from a linear fit to the identified positions for the events with (*c*) two tracks and (*d*) more than two tracks. The distributions from antihydrogen annihilations are shown in solid black lines and from cosmic rays in dotted red lines. The shaded regions in (*b*), (*c*), and (*d*) indicate the range of parameters that are rejected.

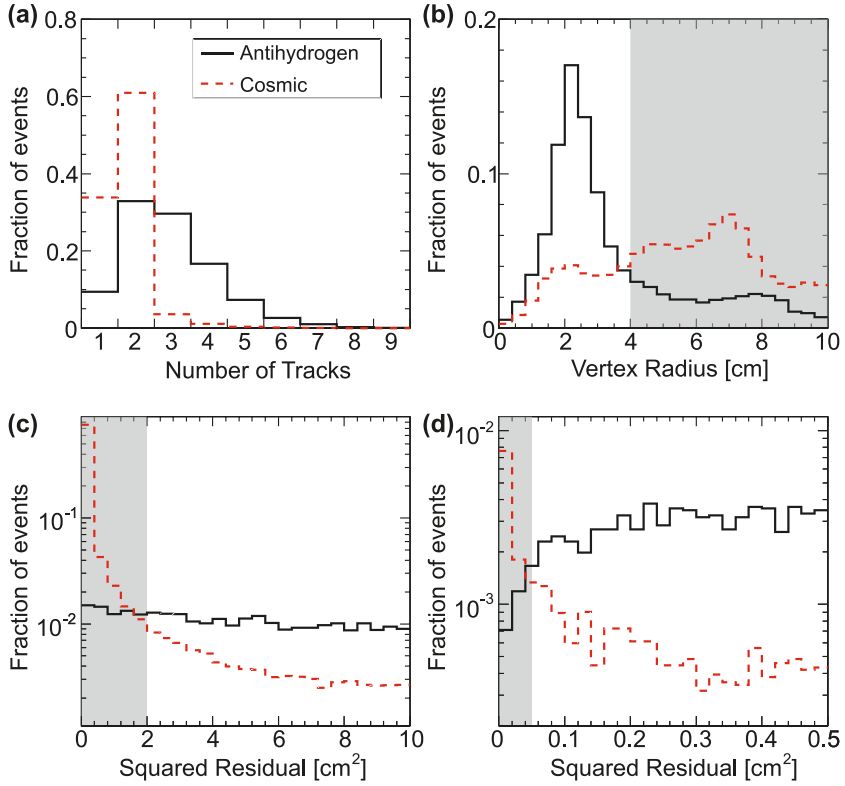

tected, and (*b*) a cosmic event. The reconstruction algorithm has fitted a vertex to the cosmic event, however, as will be detailed later, we can use details of the topology to distinguish between the cosmic events and the antiproton events. Apart from fully reconstructed events we also use an annihilation detector trigger, signaling events a minimum of two silicon modules. This trigger has an efficiency for antiproton annihilations of ∼85%, however, to identify the fraction of these events that are antihydrogen we need the reconstructed vertices as detailed earlier.

Fig. 8. Clearing of antiprotons from the magnetic trap before de-energizing it. (*a*) Magnetic field strength on axis and the axial electric potential used to clear particles to the left. (*b*) Effective potential calculated for antiprotons in the superposed fields shown in (*a*) with different transverse kinetic energies. Above ~20 eV transverse kinetic energy the electric field is no longer strong enough prevent some particles from remaining.

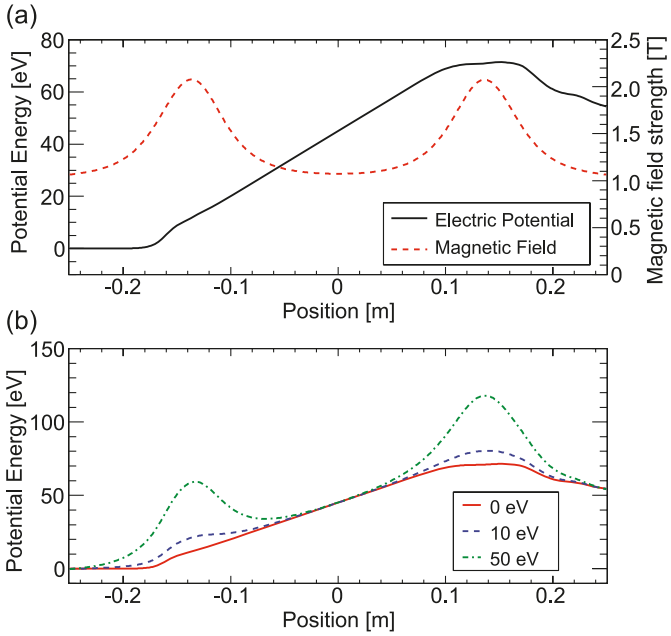

5. Trapping

Towards the end of 2009 we carried out a series of 212 trapping attempts. The antiproton clouds used for these experiments were 0.8 mm in radius and typically contained 40 000 antiprotons with a temperature of 358±55 K measured before injection into the positrons. The positron plasma had a radius of 1.0 mm and and a density of 7×10^7 cm^{-3} at a temperature of 71±10 K. Upon injection of the antiprotons the temperature of the positrons increased to 194±23 K.

Before merging, the two particle species we energized the magnetic-minimum trap to a depth of 0.5 K. We then merged the two species for 1 s and observed 2700±700 annihilation detector counts. Analysing the spatial distribution of these annihilations in the same way as we did in ref. 9, we estimate that about 80% of the triggers stem from antihydrogen that annihilated directly on the inner surfaces of the traps. The remaining 20% of the annihilations stemmed from antihydrogen that is field ionized before reaching the wall of the apparatus, creating an antiproton that is then lost on the wall, as it is beyond the critical radius caused by the octupole field. We distinguish these two types of annihilations by fitting the axial spatial distribution of the annihilations [9]. Antihydrogen that does not field-ionize can potentially be trapped. To look for trapped antihydrogen we clear out all remaining charged particles at the end of the 1 s mixing time, and then abruptly turn off the magnetic minimum trap. Our magnets have been designed such that we can de-energize them by dumping their energy in an external resistor network. This feature forms an integral part of the quench protection system of the magnets, but the fast de-energizing can also be triggered at will. Figure 6 shows the current in three trap magnets as a function of time. The e-folding time of the current decay is 9 ms. We searched for trapped particles in a 30 ms window after triggering the fast shut down, or equivalently until the trap depth has been reduced to below 1% of its initial value.

6. Backgrounds for trapping

Before discussing what was observed in the trapping experiments, we consider the possible backgrounds or fake events that may arise in the experiment.

6. 1 Cosmics

Our annihilation detector also detects cosmic rays. To separate cosmic events from true annihilations we make cuts on the topology of the events. Figure 7 summarizes the different cuts we apply. The particles we observe from cosmic rays are typically high energy and we therefore discriminate using the curvature of the tracks forming the vertex. We also consider the number of tracks composing a vertex as well as the degree of overlap of the tracks and the vertex. The latter is done by cutting on the residual, which is the distance of all the tracks from the estimated vertex. Finally, we also discard events based upon the radial position of the vertex, deeming it a reconstructed annihilation of a cosmic if the radius is significantly beyond the size of the trap. The cuts were refined by applying them to large samples of both cosmic and antihydrogen formation events. We optimized for the maximum amount of cosmic rejection while trying to retain as many annihilation events as possible. The final result was a cosmic rejection of 99.5% while retaining an over all efficiency of annihilation vertices of (40±7)%. The cuts were applied to events in the 30 ms trapping window only after they had been thus decided upon.

For the 2009 series of runs the expected cosmic background was 0.14 events in 212 runs. Six annihilations (passing all the cuts) wereobserved. The probability of this observation being due to fluctuations in the cosmic background is 9.2×10^{-9}, corresponding to a significance of 5.6 standard deviations. We thus concluded that we have observed antiproton annihilations upon de-energizing our magnetic-minimum trap in these experiments. However, as it turns out, a more important background remains; mirror-trapped antiprotons.

6.2 Mirror-trapped antiprotons

As our detector cannot distinguish between antiproton and antihydrogen events we cannot a priori tell if the six observed events were in fact antihydrogen or bare antiprotons. The strong rejection of cosmics has convinced us that we did observe antiproton annihilations, but that does not automatically imply that they were due to antihydrogen.

As briefly mentioned earlier, we eject all charged particles from the trap before de-energizing the magnets and looking for annihilations. Bare antiprotons can be trapped by the magnetic fields due to their gyromagnetic moment. An antiproton with momentum transverse to the magnetic field will have a magnetic moment given by

$$\mu\bar{p} = \frac{E_\perp}{|\mathbf{B}|} \qquad (2)$$

Fig. 9. The time after the start of the magnet shutdown and z-position relative to the centre of the trap of the simulated annihilations of (*a*) mirror-trapped antiprotons and (*b*) antihydrogen atoms released from the magnetic trap. Individual simulated annihilations are shown as discrete points. The lines show the contours of constant density, which contain 50% (green) and 99% (red) of the density when convolved with the resolution of the detector. The solid diamond-shaped points mark the positions of the six candidate events identified in the trapping experiment. Some mirror-trapped antiprotons impacted at ±14 cm, where a step in the radius of the electrodes occurs.

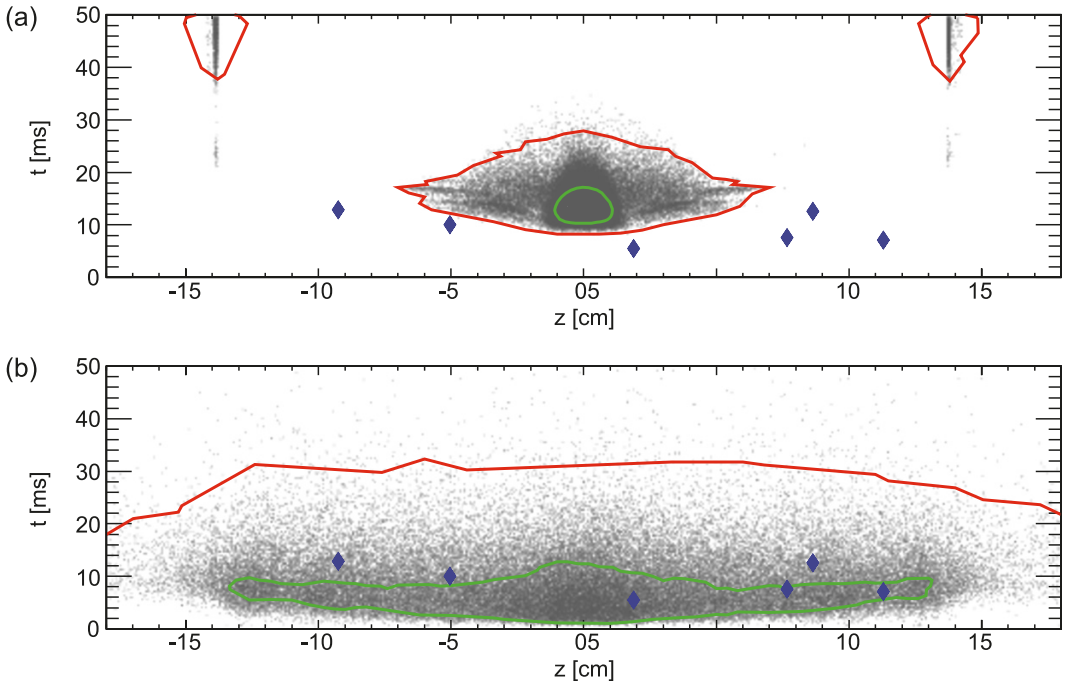

where $E_\perp$ is the kinetic energy of the particle in the plane transverse to the local magnetic field and **B** is the magnetic field. This magnetic moment is adiabatically conserved. If the magnetic field varies along the trajectory of the particle, energy is exchanged between the axial and transverse motions such that the magnetic moment remains constant. If the magnetic field at some point along the trajectory is strong enough with respect to thae field at the starting position of the particle, all axial energy is removed such that the particle reaches a turning, or reflection, point. This effect is called "mirror-trapping."

We cleared the charged particles that remained in the magnetic-minimum trap by a series of pulses of an average field of ~2.5 V/cm applied for 10 ms. For the first few pulses we observed annihilations corresponding to a few tens of antiprotons, but for the last pulses we no longer saw any ejected antiprotons. This demonstrated that antiprotons can indeed become mirror trapped, and that they can be efficiently ejected.

However, as Fig. 8 shows, the clearing fields we applied cannot eject arbitrarily energetic antiprotons. If an antiproton has a $E_\perp$ larger than 20 eV it will not be cleared by our fields. This is a very large energy compared to the typical temperatures of our particles in the mixing trap. Collisions or energetic antiprotons remaining from the catching procedure could in principle supply such energetic antiprotons, however, estimates show this to be unlikely [19]. A less calculable risk is that an experimental error or failing equipment caused our experiment to perform sub-optimally in such a way as to be a source of energetic antiprotons. As we have not experimentally distinguished antiprotons from antihydrogen, we have not experimentally demonstrated that the events are a result of trapped antihydrogen.

To try to address this problem we have undertaken a series of simulations of the dynamics of antiprotons and antihydrogen atoms during the de-energization of the magnetic trap, as detailed in ref. 19. In the code, particles are given an initial position and velocity from a pre-selected distribution, and their trajectories are calculated using the full 3D Lorentz force based on the known magnetic and electric fields present in the system. We used these simulations to investigate the efficiency of the clearing fields discussed above and found that, independent of the initial position of the particles in the trap, the upper limit of $E_\perp$ that can be cleared is 20 eV, as estimated from the simple on-axis effective potential calculations shown in Fig. 8. Further the simulations were used to model the distribution in position and time of annihilations occurring during the de-energization.

Figure 9 shows the results of these simulations overlayed with the six annihilation events we observed during our 212 trapping search experiments. The distribution of released mirror-trapped antiprotons depends upon the energy distribution assumed, but the example shown is representative. As it turns out, the main features are not overly sensitive to the initial parameters. The figure shows that mirror-trapped antiprotons preferentially emerge in the axial centre of the trap, with some peaks at ±14 cm where there is an inward radial step in the electrode radius. Contrary to this, antihydrogen emerges fairly smoothly along the axis, and somewhat earlier during the de-energization. Details of the calculations are given in ref. 19.

The distinctly different features of antihydrogen and mirror-trapped antiproton loss can be understood intuitively by reflecting on their respective initial conditions. Antihydrogen held in our trap has a kinetic energy less than the equiv-

alent of 0.5 K. An antihydrogen atom with this energy will, depending on its initial momentum bounce relatively few times before it can escape from the trap while the trap is de-energized. Thus, the de-energization is quasi-instantaneous for trapped antihydrogen, which means that it will emerge quasi-isotropically as observed in the simulations. For antiprotons the situation is quite different. The antiprotons that survive the clearing are likely to be of electron-Volt kinetic energy, and will thus undergo many bounces during the de-energization and it is thus much more likely that they be lost at points where the trap is particularly shallow. Antiprotons tend to follow field-lines, and as it turns out, their trajectories mean that they escape to annihilate nearer to the axial centre. A caveat to this argument when dealing with real data rather than simulations is that since we do not know for certain the source of mirror-trapped antiprotons, if indeed any remain after clearing, we cannot necessarily expect the argument for these to hold.

The six observed events overlap well with the antihydrogen-release distribution and very poorly with that of mirror-trapped antiprotons. We conclude that the six events are strong candidates for being caused by trapped antihydrogen atoms.

7. Conclusions

We have presented the recent progress of the ALPHA collaboration towards trapping of antihydrogen. Because of the shallow trap, the main obstacle is to make antihydrogen cold enough to trap. We have discussed how the magnetic fields used to form the trap for the neutral antihydrogen atoms impose constraints on the properties of the particle ensembles we can use for making antihydrogen. We further discussed how ALPHA has overcome these obstacles and produced antihydrogen inside the neutral atom trap, with temperatures and densities unperturbed by the added magnetic trap fields. The temperatures are still two orders of magnitude larger than the trap depth for ground state antihydrogen, but theoretical estimates have indicated that a small fraction of trappable antihydrogen could still be made.

During 212 trapping experiments we observed six candidate events. We have argued that the observed candidate events are indeed antiproton annihilations and not cosmic background in our annihilation detector. We further demonstrate how we have cleared out mirror-trapped antiprotons and what the limitations in this regard are. Our annihilation detector cannot distinguish, on an event-by-event basis, between antiproton and antihydrogen annihilations, as we do not detect the gamma photons stemming from the positron annihilation in an antihydrogen annihilation. Instead, we have simulated how the antiprotons and antihydrogen escape differently once the magnetic trap is de-energized, and found that the six candidate events are compatible with simulated distributions of antihydrogen atoms and not with mirror-trapped antiprotons. However, without knowing how well the simulations performed represent the real experiment, or an unambiguous control experiment, we cannot yet definitively claim to have observed trapped antihydrogen.

To further increase the number of cold antihydrogen in future experiments, something that would greatly improve the likelihood of trapping, we have recently implemented evaporative cooling of the antiprotons, and managed to cool clouds of these to $\sim$9 K [17]. However, as mentioned earlier, the positron temperature is currently the dominating factor and we have, therefore, not yet applied this technique in trapping experiments. We think the positron temperature is currently limited by electronic noise, among other things, and are actively pursuing ways to reduce this further. With colder positrons and antiprotons and improved experimental cross-checks, we believe that we will soon be in a position to demonstrate the first trapping of antihydrogen.

References

1. G.M. Shore. Nucl. Phys, **B717**, 86 (2005). doi:10.1016/j.nuclphysb.2005.03.040.
2. M. Amoretti, C. Amsler, G. Bonomi, A. Bouchta, P. Bowe, C. Carraro, C.L. Cesar, M. Charlton, M.J. Collier, M. Doser, V. Filippini, K.S. Fine, A. Fontana, M.C. Fujiwara, R. Funakoshi, P. Genova, J.S. Hangst, R.S. Hayano, M.H. Holzscheiter, L.V. Jørgensen, V. Lagomarsino, R. Landua, D. Lindelöf, E. Lodi Rizzini, M. Macrì, N. Madsen, G. Manuzio, M. Marchesotti, P. Montagna, H. Pruys, C. Regenfus, P. Riedler, J. Rochet, A. Rotondi, G. Rouleau, G. Testera, A. Variola, T.L. Watson, and D.P. van der Werf; ATHENA Collaboration. Nature, **419**, 456 (2002). doi:10.1038/nature01096. PMID:12368849.
3. G. Gabrielse, N.S. Bowden, P. Oxley, A. Speck, C.H. Storry, J.N. Tan, M. Wessels, D. Grzonka, W. Oelert, G. Schepers, T. Sefzick, J. Walz, H. Pittner, T.W. Hänsch, and E.A. Hessels; ATRAP Collaboration. Phys. Rev. Lett. **89**, 213401 (2002). doi:10.1103/PhysRevLett.89.213401.
4. W. Bertsche, A. Boston, P. Bowe, C. Cesar, S. Chapman, M. Charlton, M. Chartier, A. Deutsch, J. Fajans, and M. Fujiwara; ALPHA Collaboration. Nucl. Inst. Meth. A, **566**, 746 (2006). doi:10.1016/j.nima.2006.07.012.
5. N. Madsen, M. Amoretti, C. Amsler, G. Bonomi, P.D. Bowe, C. Carraro, C.L. Cesar, M. Charlton, M. Doser, A. Fontana, M.C. Fujiwara, R. Funakoshi, P. Genova, J.S. Hangst, R.S. Hayano, L.V. Jørgensen, A. Kellerbauer, V. Lagomarsino, R. Landua, E. Lodi-Rizzini, M. Macri, D. Mitchard, P. Montagna, H. Pruys, C. Regenfus, A. Rotondi, G. Testera, A. Variola, L. Venturelli, D.P. van der Werf, Y. Yamazaki, and N. Zurlo; ATHENA Collaboration. Phys. Rev. Lett. **94**, 033403 (2005). doi:10.1103/PhysRevLett.94.033403. PMID:15698264.
6. G. Gabrielse, A. Speck, C.H. Storry, D. LeSage, N. Guise, D. Grzonka, W. Oelert, G. Schepers, T. Sefzick, H. Pittner, J. Walz, T.W. Hänsch, D. Comeau, and E.A. Hessels; ATRAP Collaboration. Phys. Rev. Lett. **93**, 073401 (2004). doi:10.1103/PhysRevLett.93.073401. PMID:15324235.
7. J. Fajans, W. Bertsche, K. Burke, S.F. Chapman, and D.P. van der Werf. Phys. Rev. Lett. **95**, 155001 (2005). doi:10.1103/PhysRevLett.95.155001. PMID:16241731.
8. M. Amoretti, et al.;ATHENA Collaboration. Phys. Lett. **578B**, 23 (2004). doi:10.1016/j.physletb.2003.10.062.
9. G.B. Andresen, W. Bertsche, P.D. Bowe, C. Bray, E. Butler, C.L. Cesar, S. Chapman, M. Charlton, J. Fajans, and M.C. Fujiwara; ALPHA Collaboration. Phys. Lett. **685B**, 141 (2010). doi:10.1016/j.physletb.2010.01.066.
10. T.J. Murphy and C.M. Surko. Phys. Rev. A, **46**, 5696 (1992). doi:10.1103/PhysRevA.46.5696. PMID:9908819.
11. S. Maury. Hyperfine Interact. **109**, 43 (1997). doi:10.1023/A:1012632812327.
12. G.B. Andresen, W. Bertsche, P.D. Bowe, C.C. Bray, E. But-

ler, C.L. Cesar, S. Chapman, M. Charlton, J. Fajans, M.C. Fujiwara, D.R. Gill, J.S. Hangst, W.N. Hardy, R.S. Hayano, M.E. Hayden, A.J. Humphries, R. Hydomako, L.V. Jørgensen, S.J. Kerrigan, L. Kurchaninov, R. Lambo, N. Madsen, P. Nolan, K. Olchanski, A. Olin, A.P. Povilus, P. Pusa, E. Sarid, S. Seif El Nasr, D.M. Silveira, J.W. Storey, R.I. Thompson, D.P. van der Werf, and Y. Yamazaki; ALPHA Collaboration. Rev. Sci. Instrum. **80**, 123701 (2009) . doi:10.1063/1.3266967. PMID:20073120.

13. G.B. Andresen, W. Bertsche, P.D. Bowe, C.C. Bray, E. Butler, C.L. Cesar, S. Chapman, M. Charlton, J. Fajans, M.C. Fujiwara, R. Funakoshi, D.R. Gill, J.S. Hangst, W.N. Hardy, R.S. Hayano, M.E. Hayden, R. Hydomako, M.J. Jenkins, L.V. Jørgensen, L. Kurchaninov, R. Lambo, N. Madsen, P. Nolan, K. Olchanski, A. Olin, A. Povilus, P. Pusa, F. Robicheaux, E. Sarid, S.S. El Nasr, D.M. Silveira, J.W. Storey, R.I. Thompson, D.P. van der Werf, J.S. Wurtele, and Y. Yamazaki; ALPHA Collaboration. Phys. Rev. Lett. **100**, 203401 (2008). doi:10.1103/PhysRevLett.100.203401. PMID:18518531.
14. F. Robicheaux. Phys. Rev. A, **70**, 022510 (2004). doi:10.1103/PhysRevA.70.022510.
15. J. Fajans, N. Madsen, and F. Robicheaux. Phys. Plasmas, **15**, 032108 (2008). doi:10.1063/1.2899306.
16. D.L. Eggleston, C.F. Driscoll, B.R. Beck, A.W. Hyatt, and J.H. Malmberg. Phys. Fluids B, **4**, 3432 (1992). doi:10.1063/1.860399.
17. G.B. Andresen, M.D. Ashkezari, M. Baquero-Ruiz, W. Bertsche, P.D. Bowe, E. Butler, C.L. Cesar, S. Chapman, M. Charlton, J. Fajans, T. Friesen, M.C. Fujiwara, D.R. Gill, J.S. Hangst, W.N. Hardy, R.S. Hayano, M.E. Hayden, A. Humphries, R. Hydomako, S. Jonsell, L. Kurchaninov, R. Lambo, N. Madsen, S. Menary, P. Nolan, K. Olchanski, A. Olin, A. Povilus, P. Pusa, F. Robicheaux, E. Sarid, D.M. Silveira, C. So, J.W. Storey, R.I. Thompson, D.P. van der Werf, D. Wilding, J.S. Wurtele, and Y. Yamazaki; ALPHA Collaboration. Phys. Rev. Lett. **105**, 013003 (2010). doi:10.1103/PhysRevLett.105.013003. PMID:20867439.
18. M.C. Fujiwara. AIP Conf. Proc. **793**, 111 (2005).
19. G.B. Andresen, M.D. Ashkezari, M. Baquero-Ruiz, W. Bertsche, P.D. Bowe, C.C. Bray, E. Butler, C.L. Cesar, S. Chapman, and M. Charlton; ALPHA Collaboration. Physics Letters B. In press. (2010). doi:10.1016/j.physletb.2010.11.004.